Surface-induced nematic order variation: Intrinsic anchoring and subsurface director deformations

G. Skačej,[1] A. L. Alexe-Ionescu,[2] G. Barbero,[3] and S. Žumer[1]
[1]*Physics Department, University of Ljubljana, Jadranska 19, SI-1000 Ljubljana, Slovenia*
[2]*Department of Physics, ''Politehnica'' University of Bucharest, Splaiul Independentei 313, R-77206 Bucharest, Romania*
[3]*Dipartimento di Fisica del Politecnico di Torino, Corso Duca degli Abruzzi 24, I-10129 Torino, Italy*
(Received 11 July 1997)

The nematic orientation close to a solid substrate is investigated by means of a Landau–de Gennes phenomenological model. We show that a spatial variation of the scalar order parameter induces a subsurface variation of the average molecular orientation and an intrinsic contribution to the anchoring when the splay and bend elastic constants are different from the twist elastic constant. A quasi-splay-bend elastic constant is deduced by comparing the surface term proportional to the first derivative of the tilt angle with the one proposed long ago by Nehring and Saupe [J. Chem. Phys. **54**, 337 (1971); **56**, 5527 (1972)]. The effective anchoring being a combination of the external contribution originating from the interaction with the substrate and the intrinsic anchoring energy resulting from the spatial variation of the scalar order parameter is analyzed. Matching elastic and magnetic effects on a nematic slab, the corresponding effective extrapolation lengths are estimated. [S1063-651X(98)00102-0]

PACS number(s): 61.30.Cz, 61.30.Gd

I. INTRODUCTION

In bulk nematic phases intermolecular interactions responsible for the nematic order tend to orient molecular long axes $\vec{a}$ parallel to a common direction $\vec{n}$, called the director [1]. Therefore, in a slab of nematic material confined by surfaces that impose the same molecular orientation one would expect a homogeneous nematic orientation. In contrast, some experimental investigations [2–4] show that liquid-crystal molecules in the surface layer can have an orientation different from that in the bulk material. Also, a little more detailed theoretical analysis immediately shows that nontrivial ordering close to the surface is possible. Theoretical predictions about subsurface deformations have been published by different groups, mainly in connection with the splay-bend (K_{13}) elastic constant introduced long ago by Nehring and Saupe [5,6]. Barbero *et al.* [7] realized that the inclusion of the K_{13} term in the Frank elastic energy density responsible for deformed ordering close to the surface requires an additional term proportional to the square of the second derivative of the angle characterizing the nematic director field (second-order elasticity) to prevent its infinite distortion. In this approach a strong and very localized but finite subsurface deformation of the nematic director field is described in terms of the splay-bend elastic constant K_{13} and the effective second-order elastic constant K^* [7–10]. Possible variations of the nematic order are not taken into account and the scalar order parameter is tacitly assumed to be constant. Although based on elastic theory, this description yields strong subsurface deformations, which raise many questions [11]. Recent, more detailed macroscopic considerations that indicate $K_{13}=0$ [12,13] apparently solve the problem of strong subsurface deformations in the macroscopic description, but do not answer the question about deformations on the molecular level [2–4].

In a completely molecular picture, nematic ordering can be deduced only for very limited and simplified systems. Recently, it has been shown using a simple lattice model that subsurface deformations can be understood in terms of a competition between external and intrinsic anchoring of the liquid crystal on the substrate and that they can be rather weak if anchoring has a normal strength [14]. A given form for the intermolecular interaction is supposed and the total energy is then deduced by summing all the intermolecular interactions [14–17]. In all these studies a zero-temperature approach (perfect nematic order) neglecting the effect of fluctuations has been used. A conclusion about the existence of subsurface deformations similar to that in Ref. [14] is coming from the density-functional approach [18].

Molecular-dynamics simulations of particles interacting via a Gay-Berne potential [19] show a substrate-induced spatial variation of the nematic scalar order parameter and molecular density (smectic ordering) [20–23]. The nematic director and the scalar order parameter are deduced by averaging molecular quantities. Unfortunately, for computational reasons the number of particles cannot be very large.

The aim of our paper is to analyze the nematic orientation close to a solid surface using the Landau–de Gennes phenomenological theory [24]. A nematic liquid crystal is described with a uniaxial order parameter that incorporates the nematic director $\vec{n}$ and the nematic scalar order parameter S [24]. We show that even if the expansion includes only terms up to the second power of the first derivatives of the order parameter, the spatial variation of S near the bounding walls yields a subsurface deformation in the nematic director and vice versa. Some of the results limited to the strong-anchoring case have been obtained recently by Vissenberg *et al.* [25] using the same phenomenological approach. Further, we show that the variation in order also results in an addition to the anchoring strength, which becomes evident only if weak anchoring is assumed. Another analysis similar to Ref. [25], but without the strong-anchoring assumption,

has been performed by Teixeira *et al.* [26], studying anchoring transitions in a nematic liquid crystal. However, this study does not present a reliable method for the determination of the anchoring energy. Therefore, our aim is to present a method which we believe is generally convenient.

Our paper is organized as follows. In Sec. II the classical Landau–de Gennes free-energy density is recalled and the number of ''elastic parameters'' entering into the model is discussed [27]. The quasi-splay-bend elastic constant and the intrinsic anchoring energy due to the spatial variation of the scalar order parameter are deduced in an approximate way in Sec. III. Numerical solutions of the planar variational problem connected with the phenomenological free-energy density written in terms of the scalar order parameters and the tilt angle formed by the nematic director $\vec{n}$ and the geometrical normal are presented in Sec. IV. We conclude in Sec. V.

II. LANDAU–DE GENNES PHENOMENOLOGICAL MODEL

In order to be able to estimate the influence of the coupling between order-parameter variation and director deformation we must briefly go through the derivation of the Landau–de Gennes free energy. A nematic liquid crystal is a ''quadrupolar'' material, which is, in the most general case, characterized by the tensor order parameter [1]

$$Q_{ij}=\frac{3}{2}S\left(n_in_j-\frac{1}{3}\delta_{ij}\right)+3P(l_il_j-m_im_j) \tag{1}$$

having quadrupolar symmetry. Here n_i stands for the ith component of the director, while l_i and m_i are components of the unit vectors that form an orthonormal triad together with $\vec{n}$. S is the uniaxial scalar order parameter and P is a scalar quantity measuring the biaxiality of the nematic. In our analysis we will, for simplicity, assume the system to be uniaxial and hence $P=0$. We expect that this simplification will not significantly affect the qualitative character of our results.

If the nematic is distorted, Q_{ij} is position dependent. The free-energy density f of the nematic is a function of Q_{ij}. If Q_{ij} changes slowly across the sample, the first spatial derivatives of Q_{ij} are small quantities. In this framework f can be expanded only up to the second order in the derivatives $Q_{ij,k}=\partial Q_{ij}/\partial x_k$ [24]:

$$f=f_0+\frac{1}{2}L_1Q_{ij,k}Q_{ij,k}+\frac{1}{2}L_2Q_{ij,j}Q_{ik,k}+\frac{1}{2}L_3Q_{ij,k}Q_{ik,j}, \tag{2}$$

where L_1, L_2, and L_3 are the ''elastic parameters'' entering the phenomenological model. f_0, given by [1]

$$f_0=\frac{1}{2}a(T-T^*)S^2-\frac{1}{3}BS^3+\frac{1}{4}CS^4, \tag{3}$$

is the free energy of the uniform ground state of the unperturbed liquid crystal. Expression (3) describes the first-order nematic-to-isotropic transition at $T_c=T^*+2B^2/9aC$. The Landau coefficients for a typical liquid crystal (4′-pentyl-4-cyanobiphenyl) are $a=0.13\times10^6$ J/m^{3}K, $B=1.6\times10^6$ J/m^3, $C=3.9\times10^6$ J/m^3, and $T_c\approx35.1$ °C [28]. For a deformed state $f\geqslant f_0$ is expected; therefore, in Eq. (2) there are no linear terms in the first-order derivative of Q_{ij} and further all terms quadratic in $Q_{ij,k}$ are assumed to be positive definite. This yields the restrictions $L_1>0$ and $L_2+L_3>-\frac{3}{2}L_1$ [24]. Using Eq. (1) and taking into account that $\vec{n}\cdot\vec{n}=1$ and hence $n_in_{i,j}=0$, it is possible to rewrite f given by Eq. (2) as [24]

$$\begin{aligned}f=f_0(S)+\frac{3}{8}\Bigg\{&\left[2L_1+\frac{1}{3}(L_2+L_3)\right](\vec{\nabla}S)^2+(L_2+L_3)\\&\times(\vec{n}\cdot\vec{\nabla}S)^2\Bigg\}+\frac{9}{8}S^2\{[2L_1+(L_2+L_3)](\vec{\nabla}\cdot\vec{n})^2\\&+2L_1[\vec{n}\cdot(\vec{\nabla}\times\vec{n})]^2+[2L_1+(L_2+L_3)][\vec{n}\times(\vec{\nabla}\times\vec{n})]^2\\&-(2L_1+L_3)\vec{\nabla}\cdot[\vec{n}(\vec{\nabla}\cdot\vec{n})+\vec{n}\times(\vec{\nabla}\times\vec{n})]\}\\&+\frac{3}{4}S\vec{\nabla}S\cdot\{(2L_2-L_3)\vec{n}(\vec{\nabla}\cdot\vec{n})+(L_2-2L_3)\vec{n}\times(\vec{\nabla}\times\vec{n})\}.\end{aligned} \tag{4}$$

This expression shows that f can be divided into three ''elastic terms.'' The first term corresponds to the spatial variation of S. The second one is the well-known Frank elastic energy density, which originates in the spatial variation of $\vec{n}$, including the saddle-splay contribution. In this approximation

$$K_{11}=K_{33}=\frac{9}{4}S_b^2[2L_1+(L_2+L_3)], \tag{5}$$

$$K_{22}=\frac{9}{2}S_b^2L_1, \tag{6}$$

$$K_{24}=\frac{9}{4}S_b^2(2L_1+L_3), \tag{7}$$

where S_b is the bulk value of the scalar order parameter. Finally, in Eq. (4) there is a third term connected to the spatial variation of S and $\vec{n}$.

Equations (5)–(7) show that within this approach the splay (K_{11}) and bend (K_{33}) constants are equal and different from the twist (K_{22}) elastic constant. Only in the special case $L_2+L_3=0$ all three Frank elastic constants have the same value $K_{11}=K_{22}=K_{33}=K=\frac{9}{2}S_b^2L_1$, while the value of the saddle-splay K_{24} elastic constant is still different [see Eq. (7)]. In this one-constant approximation f is given by

$$\begin{aligned}f=f_0(S)+\frac{3}{4}L_1(\vec{\nabla}S)^2+\frac{9}{4}L_1S^2\{&(\vec{\nabla}\cdot\vec{n})^2+[\vec{n}\cdot(\vec{\nabla}\times\vec{n})]^2\\&+[\vec{n}\times(\vec{\nabla}\times n)]^2\}-\frac{9}{4}L_1S^2\vec{\nabla}\cdot[\vec{n}(\vec{\nabla}\cdot\vec{n})+\vec{n}\times(\vec{\nabla}\times\vec{n})]\\&-\frac{9}{8}L_3\vec{\nabla}\cdot\{S^2[\vec{n}(\vec{\nabla}\cdot\vec{n})+\vec{n}\times(\vec{\nabla}\times\vec{n})]\},\end{aligned} \tag{8}$$

as it follows from Eq. (4).

We have rederived the well-known expressions for the Landau–de Gennes free-energy density (4) and for the elastic constants (5)–(7) [24,29]. In the rest of this section we are going to show how S variation can induce a distortion of the director field, studying a slab of nematic liquid crystal between plane parallel substrates and allowing only planar distortions. In a simple planar case, where $S=S(z)$ and $\vec{n}=\vec{n}(z)=[\sin\phi(z),0,\cos\phi(z)]$, $\phi(z)$ being the angle between $\vec{n}$ and the surface normal, Eq. (8) becomes

$$f=f_0(S)+\frac{3}{4}L_1S'^2+\frac{9}{4}L_1S^2\phi'^2, \tag{9}$$

where the prime denotes the derivative with respect to z. Note that in the planar case the last two terms in Eq. (8) vanish identically. Expression (9) has been considered by different authors, mainly to describe the influence of the spatial variation of the elastic constant on the nematic tilt angle profile $\phi(z)$ [26,30–34]. A simple analysis shows that in the strong anchoring case, in which values of ϕ at both walls of the nematic slab are the same, the $S=S(z)$ dependence does not induce any subsurface deformation. In fact, a minimum of f given by Eq. (9) corresponds to $\phi'=0$. The spatial variation of S can induce an additional $\phi(z)$ variation only if the deformation is already present.

Let us now consider a more general case in which $L_2+L_3\neq 0$, where $K_{11}=K_{33}\neq K_{22}$. In the planar geometry discussed above the free-energy density given by Eq. (4) has four terms

$$f=f_0(S)+f_1(\phi,S')+f_2(\phi',S)+f_3(\phi,\phi',S,S'), \tag{10}$$

introducing three elastic contributions (f_1,f_2,f_3). The energy term f_1 quadratic in S' depends also on ϕ:

$$f_1(\phi,S')=\frac{3}{4}L_1\left\{1+\frac{L_2+L_3}{2L_1}\left(\cos^2\phi+\frac{1}{3}\right)\right\}S'^2. \tag{11}$$

The Frank elastic term

$$f_2(\phi',S)=\frac{9}{4}L_1S^2\left\{1+\frac{L_2+L_3}{2L_1}\right\}\phi'^2 \tag{12}$$

is similar in structure to the corresponding term in Eq. (9). The third part of the free energy

$$f_3(\phi,\phi',S,S')=-\frac{3}{8}(L_2+L_3)\sin(2\phi)\phi'SS', \tag{13}$$

which is not present in the equal elastic constant case, couples variations in ϕ and S. If the substrates impose a scalar order parameter different from the bulk one, the free energy f is no longer minimized by a solution with $\phi'=0$. Hence a scalar order-parameter spatial dependence, which is usually localized near the substrates, induces a spatial variation of the tilt angle ϕ [25]. The influence of f_3 on structural transitions in nematic liquid crystals has been partially analyzed by Jérôme [35,36].

III. QUASI-SPLAY-BEND ELASTIC CONSTANT AND INTRINSIC ANCHORING ENERGY

Let us assume that the nematic sample occupies the $z>0$ half space and that in the planar one-dimensional case $S(0)=S_0$ and $\phi(0)=\phi_0$ are fixed by short-range forces. In the bulk the value of S depends only on temperature [Eq. (3)] and is denoted by S_b. Let us assume $S_b\neq S_0$. As is well known from the Landau theory for nonhomogeneous systems, $S(z)$ relaxes to S_b over a length that is of the order of the nematic-isotropic correlation length $\xi\sim\sqrt{L_1/a(T-T_c)}$ [24]. This characteristic length, however, does not apply to ϕ variations since there is no preferred orientation of nematic molecules ϕ_b in the bulk of the sample, which would be analogous to S_b. Bulk ϕ variations, i.e., bulk elastic deformations, caused by external fields or confinements, occur usually over a scale considerably larger than ξ.

In the following we show that in a nematic layer thick compared to ξ it is possible to include a spatial variation of the scalar order parameter in two additional surface energy terms, one corresponding to an intrinsic anchoring and one to a quasi-splay-bend elastic term. To show this we have to consider the second and the fourth terms of f defined in Eq. (10). The total energies per unit surface connected to these contributions are given by

$$\mathcal{W}=\int_0^\infty f_1(z)dz, \tag{14}$$

$$\mathcal{G}=\int_0^\infty f_3(z)dz. \tag{15}$$

From Eqs. (11) and (14) we obtain

$$\mathcal{W}=\frac{3}{4}L_1\left\{1+\frac{L_2+L_3}{2L_1}\left(\cos^2\phi(z^*)+\frac{1}{3}\right)\right\}\lambda\langle S'^2\rangle, \tag{16}$$

where

$$\langle S'^2\rangle=\frac{1}{\lambda}\int_0^\lambda S'^2dz, \tag{17}$$

λ being of the order of a few coherence lengths ξ. In Eq. (16) z^* is an effective distance in the range $(0,\lambda)$. Since λ is a mesoscopic length, $\mathcal{W}$ can be considered as an additional surface energy whose anisotropic part

$$f_s=\frac{1}{2}W_i\cos^2\phi(z^*) \tag{18}$$

can be interpreted as intrinsic anchoring with a strength defined by

$$W_i=\frac{3}{4}|L_2+L_3|\lambda\langle S'^2\rangle\approx\frac{3}{4}|L_2+L_3|\frac{(S_b-S_0)^2}{\lambda}$$
$$=\frac{|K_{11}-K_{22}|}{3\lambda}\left(1-\frac{S_0}{S_b}\right)^2, \tag{19}$$

assuming that $\langle S'^2\rangle\approx(S_b-S_0)^2/\lambda^2$ and taking into account Eqs. (5) and (6). The sign of L_2+L_3 determines the direction

of the easy axis, while the anchoring strength W_i is proportional just to the modulus of L_2+L_3. The Kléman–de Gennes extrapolation length $l_i=K_{11}/W_i$ [1] is then given by

$$l_i \approx \frac{3K_{11}}{|K_{11}-K_{22}|}\left(\frac{S_b}{S_b-S_0}\right)^2 \lambda \tag{20}$$

and depends strongly on the difference S_b-S_0.

Also the integral (15) of the term coupling the order and angle variations can be rewritten in an effective form

$$\mathcal{G}=-\frac{3}{16}(L_2+L_3)(S_b^2-S_0^2)[\sin(2\phi)\phi']_{z**}, \tag{21}$$

taking into account that $S(z)$ is a monotonic function, as will be shown in Sec. IV. The product $\sin(2\phi)\phi'$ is taken at some intermediate distance z^{**}. Since $0<z^{**}<\lambda$, $\mathcal{G}$ can be considered as an effective surface contribution having the functional form of the splay-bend elastic term introduced by Nehring and Saupe [5,6]. The corresponding quasi-splay-bend elastic constant is equal to

$$\tilde{K}_{13}=-\frac{3}{8}(L_2+L_3)(S_b^2-S_0^2)=\frac{K_{22}-K_{11}}{6}\left[1-\left(\frac{S_0}{S_b}\right)^2\right]. \tag{22}$$

It should be stressed that $\mathcal{G}$ is only effectively a surface term and cannot produce any divergent subsurface deformation as in the case of the ordinary K_{13} term. Essentially, it is a bulk term effective only in a thin layer of thickness λ. Therefore, the $\mathcal{G}$ term-induced subsurface deformations are stabilized by the bulk elastic terms f_1 [Eq. (11)] and f_2 [Eq. (12)]. The detailed director profile, which requires a complete solution of the free-energy minimization procedure, will be discussed in Sec. IV.

The intrinsic anchoring strength W_i given by Eq. (19) and a quasi-$\tilde{K}_{13}$ given by Eq. (22) are both temperature-dependent because both the bulk value of the scalar order parameter S_b and the length $\lambda \propto \xi$ exhibit rather a strong temperature dependence on approaching the nematic-isotropic phase transition.

According to the pseudomolecular model proposed by Vertogen, Flapper, and Dullemond [37,38] it is possible to evaluate elastic constants if the interparticle interaction $\mathcal{U}$ responsible for the nematic phase is known. The interaction energy for two molecules at $\vec{R}$ and $\vec{R}'=\vec{R}+\vec{r}$, whose orientations are $\vec{n}=\vec{n}(\vec{R})$ and $\vec{n}'=\vec{n}(\vec{R}')$ is $\mathcal{U}=\mathcal{U}(\vec{n},\vec{n}',\vec{r})=\mathcal{U}(\vec{n}\cdot\vec{n}',\vec{n}\cdot\vec{u},\vec{n}'\cdot\vec{u})$, where $\vec{u}=\vec{r}/r$. In the framework of Vertogen, Flapper, and Dullemond's model it can be shown that if $\mathcal{U}$ depends only on the relative position of $\vec{n}$ with respect to $\vec{n}'$, but not on $\vec{n}\cdot\vec{u}$ and $\vec{n}'\cdot\vec{u}$, the relations $K_{11}=K_{22}=K_{33}$ and $K_{13}=0$ hold [39]. This is in accordance with our result that the quasi-$\tilde{K}_{13}$ also vanishes for $K_{11}=K_{22}$.

IV. NUMERICAL SOLUTION OF THE VARIATIONAL PROBLEM

In the approximate analysis presented above we have shown that the effect of the spatial variation of the scalar order parameter is equivalent to an additional intrinsic anisotropic part of the surface anchoring energy and to an effective elastic term similar to the splay-bend term introduced by Nehring and Saupe. We have assumed that $S=S(z)$ is a monotonic function, which, over a distance comparable to few ξ, approaches its bulk value. In this framework we have shown that an $S=S(z)$ induces a $\phi=\phi(z)$, localized in a region where the S variation occurs, but we were not able to estimate the magnitude of the distortion. In this section we solve numerically the variational problem connected to the minimization of the total free energy of the nematic sample. We choose a nematic slab of thickness d with the confining surfaces at $z=\pm d/2$ (Fig. 1). Again the deformation is assumed to be planar.

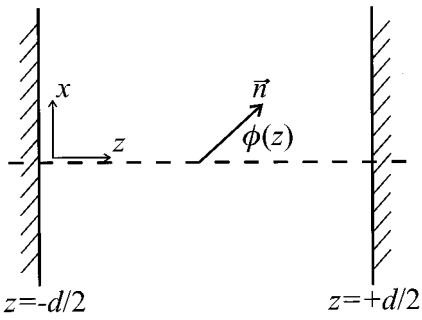

FIG. 1. Slab of nematic liquid crystal; the definition of the tilt angle $\phi(z)$.

To solve the minimization problem we first have to derive the Euler-Lagrange equations and the corresponding boundary conditions. The total free energy to be minimized can then be written as

$$F=\int_V f_B(\phi(z),\phi'(z),S(z),S'(z))dV + \int_S f_S(\phi(\pm d/2),\phi_0,S(\pm d/2),S_0)dS, \tag{23}$$

where $f_B=f_0+f_1+f_2+f_3$ and f_S are the bulk and surface free-energy densities, respectively, while ϕ_0 and S_0 denote the substrate-induced values of ϕ and S. The surface contribution f_S arising from the interaction between the nematic and the substrate is nonzero only in the weak-anchoring case. In the presence of an external field also the field energy contribution must be added to f_B.

In our case the Euler-Lagrange equations have the form

$$\frac{\partial f_B}{\partial \phi}-\frac{d}{dz}\frac{\partial f_B}{\partial \phi'}=0, \tag{24}$$

$$\frac{\partial f_B}{\partial S}-\frac{d}{dz}\frac{\partial f_B}{\partial S'}=0 \tag{25}$$

and are both of the second order. Hence there must be four boundary conditions for the above equations to present a well-defined system. In the strong-anchoring case and for a symmetric sample these read $\phi(\pm d/2)=\phi_0$ and $S(\pm d/2)=S_0$, while in the weak-anchoring case they become

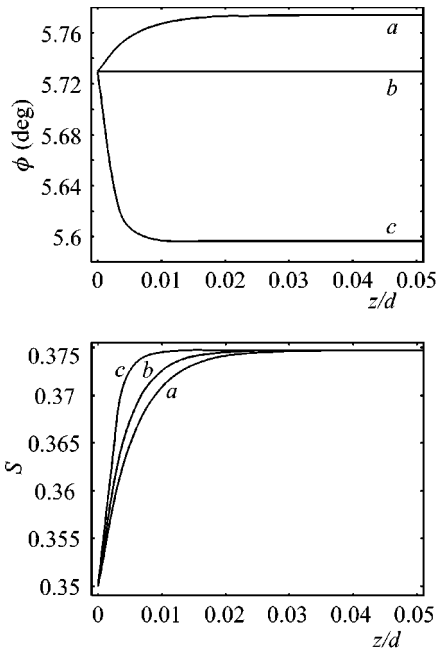

FIG. 2. Director and scalar order-parameter profiles in the strong-anchoring case; $\phi_0=0.1(180°/\pi)\approx 5.73°$, $S_b\approx 0.3747$, $S_0=0.35$, and $L_2+L_3=+L_1,0,-L_1$ (cases a, b, and c, respectively). The sample thickness is equal to $d=1\ \mu$m.

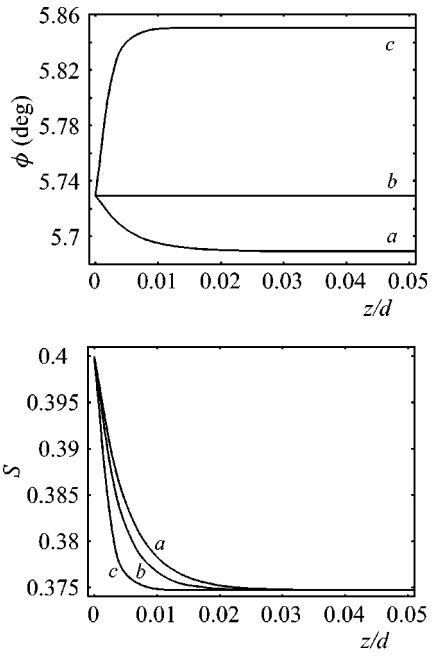

FIG. 3. Director and scalar order-parameter profiles in the strong-anchoring case; all the parameters are equal to those of Fig. 2, except $S_0=0.4$.

$$\pm\left(\frac{\partial f_B}{\partial \phi'}\right)_{z=\pm d/2}+\frac{\partial f_S}{\partial \phi(\pm\frac{d}{2})}=0, \tag{26}$$

$$\pm\left(\frac{\partial f_B}{\partial S'}\right)_{z=\pm d/2}+\frac{\partial f_S}{\partial S(\pm\frac{d}{2})}=0. \tag{27}$$

The system (24)–(27) has been solved numerically by means of the relaxation method for boundary-value problems [40]. We will first consider the case with infinitely strong anchoring and then continue with a more general case with an arbitrary strength of anchoring.

A. Strong-anchoring case

In the strong-anchoring limit at the confining surfaces the scalar order parameter S is fixed to S_0 by surface treatment, while in the bulk it takes the temperature-determined value $S_b\neq S_0$. Further, the surface tilt angle $\phi(\pm d/2)$ is fixed to ϕ_0. Although the actual surface tilt does not vary, S variation induces a subsurface deformation. Some examples of director and scalar order-parameter profiles are shown in Figs. 2 and 3. The S variation occurs in a layer whose thickness is ~ 10 nm, which is indeed of the order of ξ, as predicted by a rough estimate in Sec. III. In this region also the variation of ϕ, i.e., a subsurface deformation, occurs. We find that the amplitude of the resulting deformation $\Delta\phi$, defined as $\Delta\phi=\phi_b-\phi_0$ (ϕ_b being the bulk tilt angle), is proportional to the above-introduced quasi-$\widetilde{K}_{13}$ elastic constant, similar to the case of normal K_{13} elastic constant. If the amplitude of the S variation (i.e., S_b-S_0) is small enough to neglect the variation of the Frank elastic constant $K\propto S_b^2$ close to the interface, the same relation as for the ordinary K_{13} may be used to approximately predict the deformation amplitude $\Delta\phi$ [41]:

$$\Delta\phi\approx-\frac{\widetilde{K}_{13}}{2K}\sin 2\phi(\pm d/2). \tag{28}$$

Note that whereas the deformation stabilization in Ref. [41] is governed by second-order elasticity, it is here by the positive-definite terms $f_1\propto S'^2$ and $f_2\propto\phi'^2$ introduced in Sec. II.

The quasi-$\widetilde{K}_{13}$ elastic constant given by Eq. (22) depends on both L_2+L_3 and the difference between the bulk and the surface scalar order parameter. The numerical solutions confirm that if L_2+L_3 changes sign, the deformation amplitude $\Delta\phi\propto\widetilde{K}_{13}$ changes sign as well. If $L_2+L_3=0$, the subsurface deformation vanishes and $\Delta\phi=0$. Further, the change in sign of $\Delta\phi$ occurs if the sign of S_0-S_b is changed. From Figs. 2 and 3 it can be deduced that also the characteristic length of the subsurface distortion depends on L_2+L_3. In comparison to cases with negative L_2+L_3, positive L_2+L_3 yield larger proportionality constants in the stabilizing terms f_1 and f_2 [see Eqs. (11) and (12)], which means that stabilization effects for $L_2+L_3>0$ are stronger than for $L_2+L_3<0$. Hence the corresponding deformations are weaker, i.e., occurring over a larger distance and having smaller amplitude, the former holding for both ϕ and S profiles, while the latter is true for ϕ profiles only since S_b-S_0 is fixed if anchoring is strong.

B. Weak-anchoring case

Let us now consider a more realistic nematic-surface coupling, i.e., an anchoring situation where actual surface values $S(\pm d/2)$ and $\phi(\pm d/2)$ are allowed to vary. Any deviation

of these values from the surface-induced ones (S_0 and ϕ_0, respectively) is penalized with an increase of the anchoring energy. This short-range interaction energy is usually modeled as a contribution to the surface free energy expressed in powers of the tensor order parameter Q_{ij}. Here we use [42]

$$\mathcal{W}_S=\frac{1}{2}W_e(Q_{ij}-Q_{ij}^0)^2 \tag{29}$$

with Q_{ij}^0 as the tensor order parameter corresponding to surface preferred values of S and $\vec{n}$ (and consequently ϕ) and W_e related to the corresponding substrate (external) anchoring strength. Taking into account expression (1), Eq. (29) reads

$$\mathcal{W}_S=\frac{9}{8}W_e\left[\frac{2}{3}[S(\pm d/2)^2+S_0^2]-2S(\pm d/2)\right.$$
$$\left.\times S_0\left(\cos^2[\phi(\pm d/2)-\phi_0]-\frac{1}{3}\right)\right]. \tag{30}$$

Note that if there is no S variation, Eq. (30) reduces to the standard Rapini-Papoular expression $\mathcal{W}_S \propto -\cos^2[\phi(\pm d/2)-\phi_0]$ [43], while in cases without elastic distortion $[\phi(\pm d/2)=\phi_0]$ it has the form $\mathcal{W}_S \propto [S(\pm d/2)-S_0]^2$. In the most general case, however, S and ϕ variations are coupled in the anchoring energy (30). The weak-anchoring case has been considered previously in Ref. [32] in the one-constant approximation, in which the quasi-splay-bend elastic constant is identically zero. Now we shall generalize this analysis by allowing $L_2+L_3\neq 0$.

The same Euler-Lagrange equations as in the strong-anchoring case have been solved, however, with modified boundary conditions. As the actual surface tilt angle is not fixed anymore, effects of S-variation-induced intrinsic anchoring can now be revealed. The easy axis for this intrinsic anchoring contribution can be either planar (for $L_2+L_3>0$) or homeotropic (for $L_2+L_3<0$), as it follows from Eq. (16). The calculated director profiles confirm this prediction, which is evident from Figs. 4 and 5: for $L_2+L_3<0$ $\phi(\pm d/2)<\phi_0$ and for $L_2+L_3>0$ $\phi(\pm d/2)>\phi_0$. The subsurface deformation is still present and behaves in the same manner as in the strong-anchoring case. However, supposing the same S_b and S_0, it is weaker than in the strong-anchoring case since $|S_b-S(\pm d/2)|<|S_b-S_0|$.

It should be stressed that molecular models mentioned in Sec. III, where, for instance, the intermolecular interaction is described as a superposition of the Maier-Saupe and the induced-dipole–induced-dipole coupling, yield $L_2+L_3<0$, i.e., $K_{11}<K_{22}$ [39], which corresponds to a homeotropic easy axis in our study. Thus we are going to restrict further discussion only to cases with $L_2+L_3<0$.

C. Determination of the extrapolation length

A suitable method to estimate the strength of effective anchoring is to investigate its competition with magnetic-field effects [14]. Therefore, we add the magnetic energy term [1]

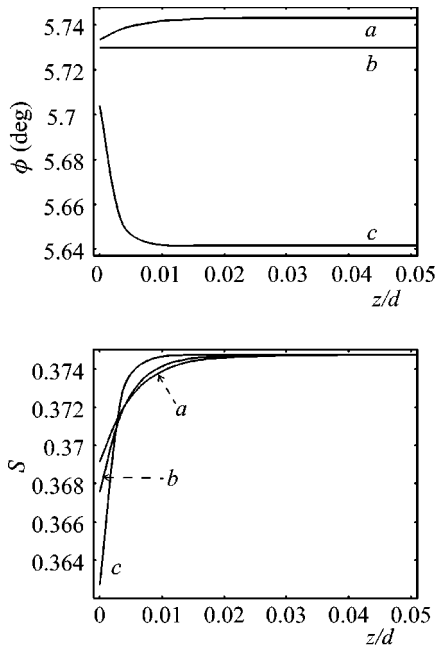

FIG. 4. Director and scalar order-parameter profiles in the weak-anchoring case; $w_e=10$, $\phi_0=0.1(180°/\pi)\approx 5.73°$, $S_b\approx 0.3747$, $S_0=0.2$, and $L_2+L_3=+L_1,0,-L_1$ (cases a, b, and c, respectively). The sample thickness is equal to $d=1\ \mu$m.

$$f_m=-\frac{1}{2}\mu_0\chi_a(\vec{n}\cdot\vec{H})^2=-\frac{1}{2}\mu_0\chi_a H^2\cos^2[\phi(z)-\alpha] \tag{31}$$

to the bulk free-energy density (10). Here H denotes the strength of the magnetic field $\vec{H}$ directed at an angle α with respect to the surface normal, μ_0 the permeability of the

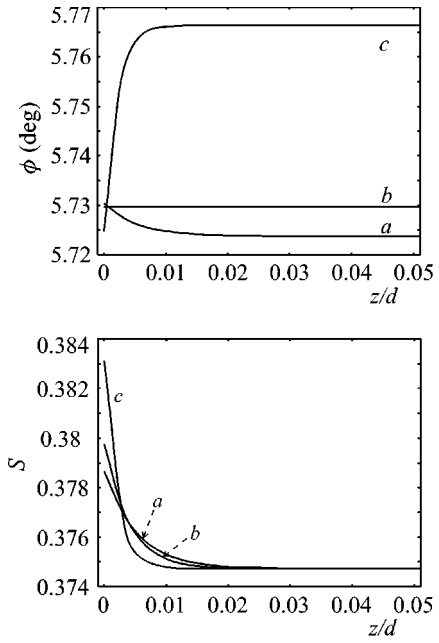

FIG. 5. Director and scalar order-parameter profiles in the weak-anchoring case; all the parameters are equal to those of Fig. 4, except $S_0=0.5$.

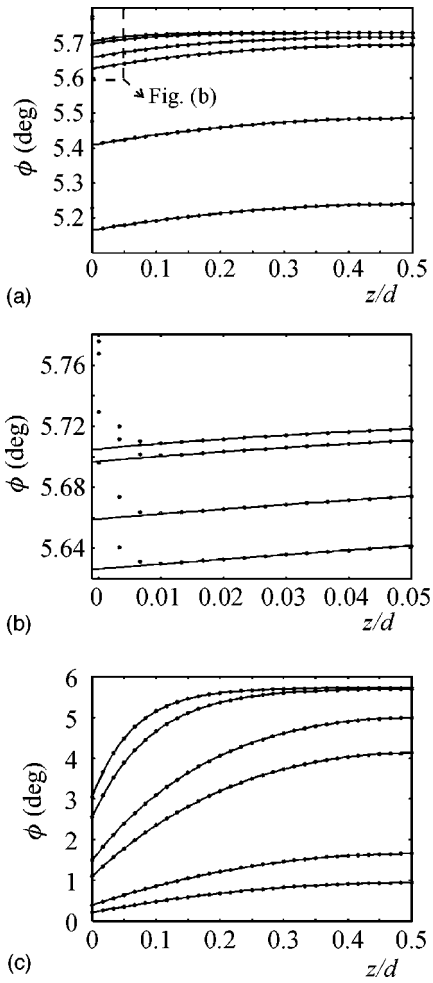

FIG. 6. Calculated director profiles (dots) in the magnetic field compared with the hyperbolic cosine fit (solid line): $w_e=5$, $L_2+L_3=-L_1$, $S_b\approx 0.3747$, and $S_0=0$ [cases (a) and (b); no external anchoring] or $S_0=0.5$ [case (c); external anchoring favoring homeotropic alignment ($\phi_0=0°$) is present]. The sample thickness is equal to $d=1\,\mu$m, the magnetic field direction $\alpha=0.1(180°/\pi)\approx 5.73°$. The magnetic-field strengths expressed in terms of the coherence length ξ_m amount to $\approx$ 65 nm, 90 nm, 205 nm, 290 nm, 650 nm, and 920 nm, the first value corresponding to the top and the last to the bottom curves of (a) and (c). Comparing cases (a) and (c), it is evident that the external anchoring is considerably stronger than the intrinsic one. (b) presents the enlarged section of (a) that is marked with a dashed line.

vacuum, and χ_a the macroscopic anisotropy of the magnetic susceptibility, which is proportional to the scalar order parameter S.

Director and scalar order-parameter profiles are again calculated by solving the Euler-Lagrange equations, which are now different from those in Secs. IV A and IV B due to the additional magnetic contribution to the bulk free energy. The influence of subsurface deformations on the large-scale director profile enters only via the effective intrinsic anchoring contribution. Therefore, ignoring the thin subsurface layer in which the subsurface deformation occurs, we can for small ϕ fit the calculated director profiles by the ansatz [see Figs. 6(a)–6(c)]

$$\phi(z)=\alpha+A\frac{\cosh(z/\xi_m)}{\cosh(d/2\xi_m)}, \tag{32}$$

the parameter A being related to the amplitude of the deformation, d the sample thickness, and ξ_m the characteristic length of this field-induced deformation, i.e., the magnetic coherence length $\xi_m=\sqrt{K/\mu_0\chi_a H^2}$ [1]. Figure 6(b) shows the enlarged subsurface region of Fig. 6(a), in which the ansatz (32) describing the macroscopic director profile fails to match the calculated profile. Since this region is of microscopic thickness (few nanometers), it will be neglected in the determination of the anchoring strength, as already stated above.

If ϕ_0 is the direction favored by the effective anchoring, the parameters of the fit (A,ξ_m) for small $\phi_0-\alpha$ yield the effective extrapolation length [14]

$$l_{eff}=\frac{K}{W_{eff}}=\left[\frac{\phi_0-\alpha}{A}-1\right]\xi_m\coth\left(\frac{d}{2\xi_m}\right). \tag{33}$$

This anchoring is a superposition of the intrinsic and external contribution. From the analysis performed in previous sections it is possible to estimate the extrapolation lengths for both sources of anchoring separately. For intrinsic anchoring we can rewrite Eq. (20) using Eqs. (5) and (6) as

$$l_i=\frac{3S_b^2}{[S_b-S(\pm\frac{d}{2})]^2}\left|\frac{2L_1}{L_2+L_3}+1\right|\lambda. \tag{34}$$

Provided λ is known, we can, using Eq. (33), compare this approximate value with the ''measured'' one. Similarly, it is possible to derive an estimate for the external anchoring extrapolation length $l_e=K_{11}/W_E$. The external anchoring strength W_E can be deduced from Eq. (30) and is given by $W_E=\frac{9}{2}W_eS(\pm d/2)S_0$, while the elastic constant K_{11} is still given by Eq. (5). In terms of the dimensionless anchoring strength $w_e=W_ed/L_1$, the length l_e can be expressed (for $S_0\neq 0$) as

$$l_e=\frac{S_b^2}{w_eS_0S(\pm\frac{d}{2})}\left[1+\frac{L_2+L_3}{2L_1}\right]d. \tag{35}$$

Assuming that both intrinsic and external anchoring have the same easy axis (e.g., homeotropic), the effective anchoring strength can be written as $W_{eff}=W_i+W_E$. Then for the corresponding extrapolation lengths the relation

$$\frac{1}{l_{eff}}=\frac{1}{l_i}+\frac{1}{l_e} \tag{36}$$

holds. If, e.g., $l_e\ll l_i$, then $l_{eff}\approx l_e$.

Let us consider a nematic slab confined by two substates treated by SiO-evaporation technique, for which $S_0=0$ can be assumed. In this case the angular dependence in Eq. (30) vanishes and hence the external anchoring in the Rapini-

TABLE I. Effective anchoring extrapolation lengths l_{eff} compared with the values l_i and l_e, predicted for intrinsic and external anchoring, respectively. All estimates for l_{eff} with $S_0=0$ refer to pure intrinsic anchoring, while the ones with $S_0=0.5$ refer to a superposition of intrinsic and external anchoring, where the latter prevails. Easy axes for both kinds of anchoring are homeotropic. The angle between the magnetic field direction and the surface normal is equal to $\alpha=0.1(180°/\pi)\approx 5.73°$, the bulk value of the order parameter to $S_b\approx 0.3747$, and the sample thickness to $d=1$ μm.

w_e	S_0	$S(\pm d/2)$	l_i	l_e (nm)	l_{eff} (nm)
1	0	0.3720	5.8×10^4 λ		4×10^5
1	0.5	0.3756	5×10^5 λ	374	375
5	0	0.3613	2.35×10^3 λ		1.67×10^4
5	0.5	0.3791	2.2×10^4 λ	74	75
10	0	0.3484	610 λ		4.3×10^3
10	0.5	0.3832	5.8×10^3 λ	37	37
50	0	0.2606	33 λ		205
50	0.5	0.4072	400 λ	7	7
100	0	0.1861	12 λ		63
100	0.5	0.4255	160 λ	3	3

Papoular sense is absent. The choice $S_0=0$ enables us therefore to investigate pure intrinsic anchoring, although $w_e\neq 0$ and thus simplifies the analysis significantly. $w_e\neq 0$ is, however, necessary to yield $S(\pm d/2)\neq S_b$, which is required for intrinsic anchoring to occur at all. However, in addition to studying cases with $S_0=0$, it will be instructive to consider also those with $S_0\neq 0$ in order to see the increase of the effective anchoring strength when external anchoring is present as well.

Director and S profiles in the magnetic field have been calculated for different values of the field strength H, the surface-imposed order parameter S_0, and the anchoring strength w_e (the example $w_e=5$ is given in Fig. 6). In all cases $L_2+L_3=-L_1$ holds, which means that $K_{11}<K_{22}$ and yields a homeotropic easy axis for the intrinsic anchoring. The Landau parameters a,B,C and the temperature were chosen such that $S_b\sim 0.3747$. The estimates for the measured effective extrapolation length are given in Table I. The results for $S_0=0$ show that if the coupling with the surface has a strength $w_e\leqslant 50$, the intrinsic anchoring is rather weak ($l_i>100$ nm). Its strength increases with increasing w_e as $S_b-S(\pm d/2)$ increases, which is in agreement with formula (34). However, if $S_0\neq 0$, the external contribution to the anchoring is nonzero as well and is, for $S_0=0.5$, e.g., considerably stronger than the weak intrinsic part [compare Figs. 6(a) and 6(c)]. Consequently, leaving other parameters unchanged, the effective extrapolation length decreases significantly in comparison to the $S_0=0$ case, and now only $w_e<5$ yields extrapolation lengths of the order of those observed experimentally (>100 nm). Since the external contribution to the effective anchoring seems to completely overwhelm the intrinsic one, we cannot expect to observe any temperature-driven anchoring transitions due to their competition.

Comparing the predicted values for l_e in cases with $S_0=0.5$ [Eq. (35)] and the measured effective ones [Eq. (33)], very good agreement is observed (see Table I), which again shows that in these cases the intrinsic anchoring is negligible with respect to the external one. Further, setting $S_0=0$ and considering the intrinsic anchoring alone, the agreement of predicted [Eq. (34)] and measured values of l_i can be achieved by setting $\lambda\approx 6-7$ nm, which is comparable to the thickness of the layer in which the S and ϕ variations occur in the absence of the magnetic field. Note also that in all cases the deformation strength of the subsurface deformation is rather small. For instance, for $w_e=5$ and $S_0=0.5$, yielding a still reasonable extrapolation length, and close to $\phi_0=\pi/4$ we obtain $d\phi/dz\sim 3\times10^{-4}\ll 1/\rho_0$ ($\rho_0\sim 1$ nm being the molecular dimension), as required by the elastic continuum theory. In this case also the variation of the order parameter is rather weak, i.e., $[S(\pm d/2)-S_b]/S_b\sim 0.01$. Cases with lower w_e yield an even smaller deformation strength.

V. CONCLUSION

In contrast to the well-known K_{13}-term-related subsurface deformations of the director field, we study here the much less known effect of the variable order parameter. A nematic liquid crystal in the slab geometry is treated using the Landau–de Gennes phenomenological theory, allowing both order and tilt angle variations. If surface and bulk values of the scalar order parameter are different and if an approximation with more than one constant is used, an intrinsic contribution to the anchoring energy is predicted. Although the free energy was expanded only up to first derivatives, the coupling between the order and tilt angle variations induces subsurface deformations similar to those caused by the ordinary K_{13} term within the second-order elastic theory [7]. The characteristic range of deformation is of the order of ξ (nematic-isotropic correlation length). In the analysis both strong- and weak-anchoring cases were treated. In the latter case the effective anchoring strength was estimated using the competition of the magnetic field and anchoring effects. The effective anchoring consists of the intrinsic and the external contribution, the external being present only if the scalar order parameter imposed by the substrate is nonzero ($S_0\neq 0$). Considering cases with $S_0\neq 0$ and with an effective extrapolation length larger than ~ 100 nm, as experimentally observed for typical substrates, the intrinsic S-variation-induced anchoring contribution is shown to be considerably weaker than the external one. For $l_{eff}\sim 100$ nm the accompanying subsurface deformation and the S variation are small, e.g., $d\phi/dz\sim 3\times10^{-4}/\rho_0$ and $[S(\pm d/2)-S_b]/S_b\sim 0.01$. It should be clearly stressed that the described phenomenological continuous approach cannot explain peculiarities in the orientation of molecules observed by Shen and co-workers [2–4] in the first molecular layer, which is in direct contact with the substrate.

ACKNOWLEDGMENTS

We wish to acknowledge the financial support of the Ministry of Science and Technology of Slovenia (Grant No. J1-7067) and from the European Union (Project INCO-Copernicus No. ERBCIC15CT960744).

[1] P. G. de Gennes and J. Prost, *The Physics of Liquid Crystals*, (Clarendon, Oxford, 1993).
[2] P. Guyot-Sionnest, H. Hsiung, and Y. R. Shen, Phys. Rev. Lett. **57**, 2963 (1986).
[3] Y. R. Shen, Liq. Cryst. **5**, 635 (1989).
[4] X. Zhuang, L. Marrucci, and Y. R. Shen, Phys. Rev. Lett. **73**, 1513 (1994).
[5] J. Nehring and A. Saupe, J. Chem. Phys. **54**, 337 (1971).
[6] J. Nehring and A. Saupe, J. Chem. Phys. **56**, 5527 (1972).
[7] G. Barbero, A. Sparavigna, and A. Strigazzi, Nuovo Cimento D **12**, 1259 (1990).
[8] S. Faetti, Phys. Rev. E **49**, 5332 (1994).
[9] S. Faetti, Liq. Cryst. **15**, 807 (1993).
[10] I. Dahl and A. de Meyere, Liq. Cryst. **18**, 683 (1995).
[11] V. M. Pergamenshchik, Phys. Rev. E **48**, 1254 (1993).
[12] S. Faetti and M. Riccardi, J. Phys. II **5**, 1165 (1995).
[13] H. Yokoyama, Phys. Rev. E **55**, 2938 (1997).
[14] G. Skačej, V. M. Pergamenshchik, A. L. Alexe-Ionescu, G. Barbero, and S. Žumer, Phys. Rev. E **56**, 571 (1997).
[15] G. Barbero, L. R. Evangelista, and S. Ponti, Phys. Rev. E **53**, 1265 (1996).
[16] P. Galatola, C. Oldano, M. Rajteri, and G. Barbero, Phys. Lett. A **210**, 101 (1996).
[17] M. Rajteri, G. Barbero, P. Galatola, C. Oldano, and S. Faetti, Phys. Rev. E **53**, 6093 (1996).
[18] P. I. C. Teixeira, Phys. Rev. E **55**, 2876 (1997).
[19] J. C. Gay and B. J. Berne, J. Chem. Phys. **74**, 3316 (1981).
[20] J. Stelzer, L. Longa, and H.-R. Trebin, J. Chem. Phys. **103**, 3098 (1995).
[21] J. Stelzer, P. Galatola, G. Barbero, and L. Longa, in *Book of Abstracts* (Freiburger Arbeitstagung Flüssigkristalle, Freiburg, 1996), P14.
[22] J. Stelzer, *Molekulardynamische Studien von Oberflächeneffekten Nematischer Flüssigkristalle* (Verlag Shaker, Aachen, 1995).
[23] Z. Zhang, A. Chakrabarti, O. G. Mouritsen, and M. J. Zuckermann, Phys. Rev. E **53**, 2461 (1996).
[24] See, for instance, E. B. Priestley, P. J. Wojtowicz, and P. Sheng, *Introduction to Liquid Crystals* (Plenum Press, New York, 1974).
[25] M. C. J. M. Vissenberg, S. Stallinga, and G. Vertogen, Phys. Rev. E **55**, 4367 (1997).
[26] P. I. C. Teixeira, T. J. Sluckin, and D. E. Sullivan, Liq. Cryst. **14**, 1243 (1993).
[27] D. W. Berreman and S. Meiboom, Phys. Rev. A **30**, 1955 (1984).
[28] H. J. Coles, Mol. Cryst. Liq. Cryst. **49**, 67 (1978).
[29] G. Vertogen and W. H. de Jeu, *Thermotropic Liquid Crystals: Fundamentals* (Springer Verlag, Berlin, 1988).
[30] G. Barbero and G. Durand, J. Appl. Phys. **69**, 6968 (1991).
[31] R. Barberi, G. Barbero, and C. Ferrero, Mol. Mater. **3**, 77 (1993).
[32] A. di Garbo and M. Nobili, Liq. Cryst. **19**, 269 (1995).
[33] A. L. Alexe-Ionescu, R. Barberi, G. Barbero, and M. Giocondo, Phys. Rev. E **49**, 5378 (1994).
[34] H. Yokoyama, S. Kobayashi, and H. Kamei, J. Appl. Phys. **61**, 4501 (1987).
[35] B. Jérôme, J. Phys.: Condens. Matter **6**, A628 (1994).
[36] B. Jérôme, Mol. Cryst. Liq. Cryst. **251**, 219 (1994).
[37] G. Vertogen, S. D. P. Flapper, and C. Dullemond, J. Chem. Phys. **76**, 616 (1982).
[38] G. Vertogen, Physica A **117**, 227 (1983).
[39] G. Barbero and L. R. Evangelista, Phys. Rev. E **56**, 6189 (1997).
[40] W. H. Press, B. P. Flannery, S. A. Teukolsky, and W. T. Vetterling, *Numerical Recipes: The Art of Scientific Computing* (Cambridge University Press, Cambridge, 1987).
[41] R. Barberi, G. Barbero, M. Giocondo, and R. Moldovan, Phys. Rev. E **50**, 2093 (1994).
[42] M. Nobili and G. Durand, Phys. Rev. A **46**, R6174 (1992).
[43] A. Rapini and M. Papoular, J. Phys. (Paris), Colloq. **30**, C4-54 (1969).